Available online at www.sciencedirect.com

ScienceDirect

www.elsevier.com/locate/jes

JES JOURNAL OF ENVIRONMENTAL SCIENCES

www.jesc.ac.cn

Natural and anthropogenic sources of lead, zinc, and nickel in sediments of Lake Izabal, Guatemala

Elisandra Hernández[1,4], *Jonathan Obrist-Farner*[1,*], *Mark Brenner*[2,3], *William F. Kenney*[3], *Jason H. Curtis*[2], *Edward Duarte*[1]

[1] *Geosciences and Geological and Petroleum Engineering Department, Missouri University of Science and Technology, Rolla, MO 65409, USA.*
[2] *Department of Geological Sciences, University of Florida, Gainesville, FL 32611, USA*
[3] *Land Use and Environmental Change Institute, University of Florida, Gainesville, FL 32611, USA*
[4] *Escuela de Química, Universidad de San Carlos de Guatemala, 01012, Guatemala*

ARTICLE INFO

Article history:
Received 7 November 2019
Revised 13 April 2020
Accepted 13 April 2020
Available online 29 May 2020

Keywords:
Lake Izabal
Heavy metals
Lead contamination
Anthropogenic impacts
Mining
Guatemala

ABSTRACT

Sediments in Lake Izabal, Guatemala, contain substantial lead (Pb), zinc (Zn), and nickel (Ni). The lack of historical data for heavy metal concentrations in the sediments makes it difficult to determine the sources or evaluate whether inputs of metals to the lake have changed through time. We measured the relative abundances and concentrations of Pb, Zn, and Ni by X-Ray Fluorescence core scanning and by Inductively Coupled Plasma Optical Emission Spectrometry in three sediment cores to explore stratigraphic distributions of metals in the lake deposits. High amounts of Pb and Zn in the core taken near the Polochic Delta suggest that galena and sphalerite mining increased Pb and Zn delivery to Lake Izabal between ~1945 and 1965 CE. An up-core Ni increase in the core taken near a different mine on the north shore of Lake Izabal suggests that recent nickel mining operations led to an increase in Ni concentrations in the local sediments, but amounts in the other cores indicate that Ni is not widely distributed throughout the lake. Sediment cores from Lake Izabal are reliable recorders of heavy metal input to the lake, and were measured to establish background metal levels, which would otherwise be unavailable. Concentrations of Pb, Zn, and Ni in older, pre-20th-century Lake Izabal sediments reflect input from natural erosion of bedrock. Our results provide previously unavailable estimates of background metal concentrations in Lake Izabal before the onset of mining. These results are necessary for future monitoring related to mining contamination of the lake ecosystem.

Introduction

Heavy metals in the environment have the potential to be toxic to biota when concentrations become sufficiently high (Jaishankar et al., 2014; Bansal and Ashtana, 2018). Recent studies found that some metals (e.g., lead [Pb], zinc [Zn], and nickel [Ni]) are common in some aquatic ecosystems, where they can be biomagnified in food webs (Bryan and Langston, 1992; Tao et al., 2012; Chatta et al., 2016; Chu et al., 2019). Organisms in Pb-contaminated ecosystems are sometimes consumed by humans and cause oxidative stress that can damage cells, nerves, brain, and kidneys (Martin and Griswold, 2009; Jaishankar et al., 2014), especially in children and pregnant women (Needleman, 1998). Exposure to Ni can

* Corresponding author.
E-mail: obristj@mst.edu (J. Obrist-Farner).

https://doi.org/10.1016/j.jes.2020.04.020
1001-0742/

Table 1 – List of Pb, Zn and Ni mines in the Lake Izabal catchment, their size, the type of extracted material, and start/end dates of mineral extraction. Numbers are associated with the mines shown in Fig. 1B.

Mine	Area (km^2)	Material extracted	Date of operation*
1. Montaña Caquipec	1	Pb, Zn, Ag	1947–1962
2. Secochoy	8	Galena, Smithsonite, Cerrusite, Pb, Ag, Zn	1999 - current
3. La Meca-1	1	Pb, Zn, Ag	1994 – current
4. Chatala	100	Ni, Pb, Zn, Ag, Au, other minerals	2005 – current
5. Extracción Minera Fénix	248	Ni, Co, other minerals	1970 – 1980/2006 – current
6. Sechol III	1	Ni, Co, Cu, Zn, Pb, Au, Ag, other minerals	2012 – current
7. Niquegua Montúfar	31	Ni, Co, other minerals	2013 – current
8. Minera Sechol	15	Ni, Co, other minerals	2013 – current
9. Selipek	38	Ni, Fe	2014 – current
10. Nabej	57	Ni, Fe, other minerals	2014 – current
11. San José del Lago	25	Ni, Co, Au, Ag, Pb, Zn, other minerals	2015 – current
12. Sebax	24	Pb, Zn, Au, Ag, Cu	2012 – current
13. Sarroguacax II	1	Pb, Zn, Ni, Cu, Au, Ag, other minerals	2007 – current
14. Llano Largo	60	Pb, Zn, Ni, Ag, Au, Co, Cu, Cd, other minerals	2007 – current

Source: Ministry of Energy and Mines, Guatemala
*The end date of mining licenses is not always reported because of extensions or administrative procedures.

cause nausea, dizziness, headache, weakness (WHO, 2005), and dermatitis (Thyssen et al., 2007). Nickel in the environment is also associated with nasal, larynx, and lung cancer (Cempel and Nikel, 2006; Goodman et al., 2011). Exposure to Zn can lead to anemia and damage to the pancreas and kidneys (ATSDR, 2005). The realization that heavy metals can cause health problems has led to efforts to reduce human exposure to such metals (e.g. elimination of Pb from gasoline, reduction of Pb concentrations in paint, plumbing systems, and ceramics, and utilization of nanoparticles to remove Ni and Zn from surface waters and soils (Goldin, 2008; Tchounwou et al., 2012; Rathor et al., 2014). Nevertheless, anthropogenic sources of metals (e.g., mining, smelting, effluent from wastewater treatment plants, industrial processes, atmospheric fallout from fossil fuel combustion, and urban runoff) and natural sources (e.g., weathering of bedrock, volcanic eruptions) persist in the environment (Nriagu and Pacyna, 1988; McIlveen and Negusanti, 1994; Rengberg et al., 1994; Heyvaert et al., 2000; ATSDR, 2005; Bradl, 2005; Thevenon et al., 2011; Tchounwou et al., 2012; Rathor et al., 2014).

Heavy metal contamination is a common problem in Guatemalan lakes and rivers. Oliva (2007) found high concentrations of Pb (41 mg/g dw (dry weight)) and chromium (Cr) (167 mg/g dw) in surface sediments from Lake Petén Itza, northern Guatemala. In the same study, she found Cr, Pb, Zn, Ni and mercury (Hg) in the endemic cichlid fish *Petenia splendida*, which is consumed by inhabitants in the region. Perez et al., 2010 analyzed three indicators of pollution and urban development in sediment cores from the same lake: Copper (Cu; ~23 μg/g), Zn (~21 μg/g), and Pb (~23 μg/g). Perez et al. (2014) found 20 μg/L of Arsenic (As) and 4.28 μg/L of Hg in water samples from Lake Atitlán, northwest Guatemala, where indigenous Maya communities drink water from the lake. Brocard et al. (2016) found a 50-fold increase (when compared to natural background levels) in Cr concentrations in Lake Chichoj, Central Guatemala, which was a result of leather tanning from an active shoe factory that has operated since 1914. These studies show that heavy metal contamination in Guatemalan lakes is a widespread problem that requires further investigation.

Pb, Zn, and Ni mining activities near Lake Izabal (Fig. 1B, Table 1) have gained substantial attention because of possible contamination of the watershed, which hosts protected forest land and endangered species. Furthermore, the lake is used as a source of food and drinking water by local communities (Aldana and Abate, 2016). The lack of baseline information on metals in the Lake Izabal water column and sediments, i.e. before mining and smelting operations in the catchment, makes it difficult to assess the impact that these activities have had, and continue to have, on the lake's ecosystem.

Several studies of surface sediments in Lake Izabal were conducted to establish the connection between mining and heavy metal concentrations. Machorro (1996) found mean concentrations of 227 μg/g of Ni, 221 μg/g of Pb, and 86 μg/g of Zn in dried surface sediments. These values were attributed to natural bedrock erosion of carbonate-hosted Pb-Zn deposits and Ni-rich laterite soils in the catchment. Pb concentrations were also tentatively attributed to Pb-Zn mine tailings located near the Cahabon River, one of the main input tributaries to Lake Izabal. Because of deteriorating water quality in Lake Izabal, Oliva (2005) and Oliva et al. (2010) began a multi-year monitoring program to assess heavy metal concentrations in the watershed and lake. They found concentrations of Pb, Zn, and Ni in surface sediments similar to those reported by Machorro (1996). Studies by Machorro (1996) and Oliva and Oliva (2005, 2010) were, however, inconclusive as to the source of metals, but mentioned several possibilities, including mining, smelting, mine tailings, natural erosion, and untreated wastewater.

We measured heavy metal concentrations in recent sediments of Lake Izabal to evaluate pre-disturbance (baseline) concentrations and to assess if recent values are linked to past and/or present mining activities in the lake catchment. We determined metal concentrations in sediments that predate the onset of mining activities in the lake catchment to: (1) evaluate if recent concentrations are similar to those observed in the past; and (2) assess if heavy metal concentrations have increased since mining activities began near Lake Izabal. We determined that the abundance of mineral deposits in the Lake Izabal's catchment, as well as mining activities at different distances from the lake, have resulted in the observed metal concentrations in the lake sediment. We also provide previously unavailable estimates of background metal concentrations, baseline information that is necessary for the agencies that are monitoring metals in the environment and are tasked with regulating impacts of current mining operations on the lake ecosystem.

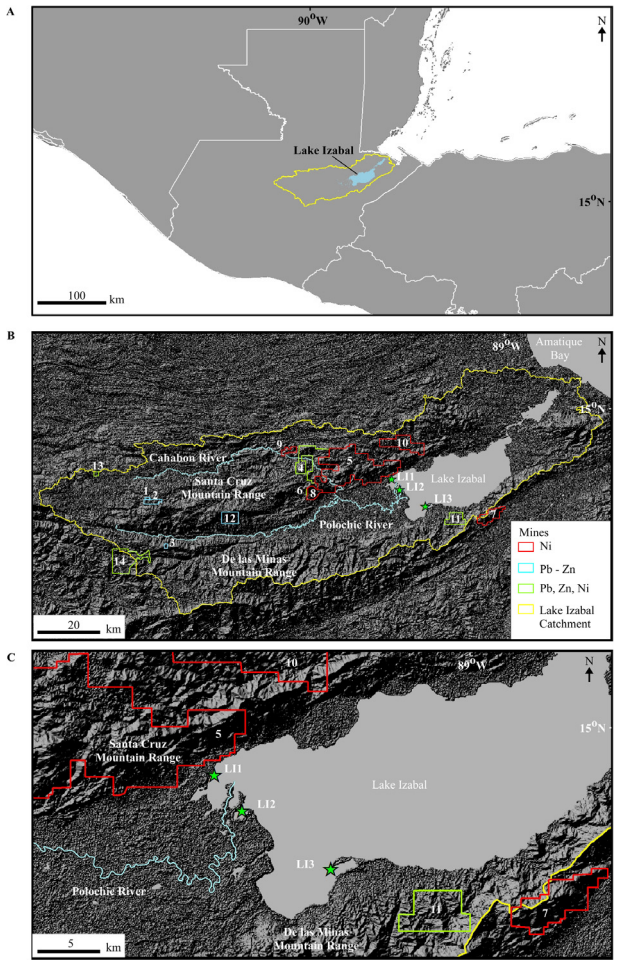

Fig. 1 – (A) Location map of the study area in Guatemala. (B) Pb, Zn and Ni mines in the Lake Izabal watershed (yellow contour) along the two main input tributaries to Lake Izabal, the Polochic and Cahabon Rivers. (C) Close-up view of the western end of Lake Izabal, showing the locations where the three study cores were collected. (For interpretation of the references to color in this figure legend, the reader is referred to the web version of this article.)

Study area

Lake Izabal is located in northeastern Guatemala (Fig. 1), has a surface area of 672 km^2, a maximum water depth of 15 m, and an estimated water residence time of 0.55 yr (Brinson and Nordlie, 1975). Izabal is the largest lake in the country and has two major rivers within its catchment, the Cahabon and Polochic (Fig. 1B). The two rivers together contribute 70%–78% of input water to the lake (Brinson, 1973; Brezonik and Fox, 1974; Brinson and Nordlie, 1975; Michot et al., 2002; Barrientos, 2005; Medina et al., 2009). The main outflow from the lake is the Dulce River, which flows from the northeast end of the lake, through another shallow basin (El Golfete; z_{max} = 4.5 m), into the Caribbean Sea. Average annual temperature in the area is 25.2 °C and mean annual precipitation is 2992 mm (Brinson, 1973; Brinson and Nordlie, 1975; Barrientos, 2005). The lake is polymictic, though a weak thermocline, which can be established during the warm rainy season (May-November), disappears rapidly with the onset of the cooler dry season (Brinson and Nordlie, 1975).

Lake Izabal is an important food and drinking water source for communities around the lake and attracts numerous visitors (Michot et al., 2002; Oliva, 2010). A large wetland at its western end is habitat for many aquatic species, migratory birds, and mammals, including the endangered West Indian manatee (Michot et al., 2002; Binimelis et al., 2007). The lake has obvious socioeconomic importance, but more than 50 years of human activity in the watershed have had measurable negative effects on the lake ecosystem (Obrist-Farner et al., 2019).

There are several mines in the Lake Izabal catchment, but only two have been heavily exploited. Montaña Caquipec (Fig. 1B; Table 1) is a Pb-Zn mine near Coban, Alta Verapaz, along the Cahabon River (ICEFI, 2014; Fig. 1B). It was active between 1947 and 1962, and when abandoned, ~100,000 mt (MT) of tailings were left behind (Van Wouw and Minaar, 2013). The second mine, Extracción Minera Fénix, located in the Santa Cruz Mountain Range (Fig. 1B; Table 1), has Ni-rich laterite soils and was exploited in the early 1960s (Brinson, 1973; Harju, 1979). Mining operations ceased in 1982 and began anew in 2013, and has produced ferronickel since then.

1. Materials and methods

We collected three sediment cores (LI1, LI2, and LI3; Fig. 1C) from Lake Izabal in June 2017, from a wooden platform mounted on plastic barrels. We used two coring devices, a mud-water interface (MWI) piston corer for the uppermost (< 1 m), unconsolidated sediments (Fisher et al., 1992) and a modified Livingstone piston corer (Livingstone, 1955) with polycarbonate core tubes for the deeper sediments. MWI cores were sectioned at 3-cm intervals in the field and placed in labeled Whirl-Pak™ bags. Deeper, more consolidated sediment sections were kept inside the polycarbonate core tubes and transported to the laboratory for analysis.

Core LI1 was collected in 3.4 m of water in the northwestern sector of the lake (15.49° N, 89.38° W; Fig. 1C). This location was chosen because of its proximity to the Ni-processing plant, which we suspected might be a source of Ni input to the water body. We collected 45 cm with the MWI corer and 88 cm with the Livingstone corer for a total core depth of 133 cm. Core LI2 was collected in 5.0 m of water near the Polochic Delta (15.45° N, 89.35° W; Fig. 1C). This location was chosen for its proximity to the Polochic River, the main tributary to the lake, to explore if upstream mining activities in the catchment have contributed metals to the lake. We collected 70 cm with the MWI corer and 435 cm with the Livingstone corer, for a total core depth of 505 cm. Core LI3 was collected in 5.7 m of water in the southwest part of the lake (15.40° N, 89.26° W; Fig. 1C). The coring location was chosen because it is far from tributaries and human activities and we consider it our "control" site. We retrieved 51 cm with the MWI corer and 404 cm with the Livingstone corer, for a total core depth of 455 cm.

Samples were shipped to the University of Florida, where intact cores in their polycarbonate tubes were run through a GeoTek multi-sensor core logger to measure sediment density and magnetic susceptibility (MS). Next, cores were cut in half lengthwise and run through the GeoTek core logger to obtain continuous, high-resolution digital images. Half of each core section was stored at the University of Florida, and the other half was shipped to Missouri University of Science and Technology (Missouri S&T) for detailed sedimentological description and geochemical analyses.

Sediment cores were dated using ^{210}Pb, ^{137}Cs, and/or ^{14}C. For ^{210}Pb and ^{137}Cs analyses, samples were dried at 60 °C for 24 h and ground to a fine powder. Weighed samples were placed in gamma tubes, sealed with epoxy glue, and allowed to

Table 2 – AMS ^{14}C dates from the LI2 core, their stratigraphic position, and the type of organic matter used for radiocarbon dating.

Depth (cm)	Sample Type	14C age ± error	Status	Modeled date (CE)
112	Plant/Wood	340 ± 15	Rejected	1942
181	Plant/Wood	165 ± 15	Accepted	1883
220	Plant/Wood	165 ± 10	Accepted	1856
394	Plant/Wood	1130 ± 15	Rejected	1737
471	Plant/Wood	135 ± 15	Accepted	1685
500	Plant/Wood	225 ± 15	Accepted	1660

Table 3 – AMS ^{14}C dates from the LI3 core, their stratigraphic position, and the type of organic matter used for radiocarbon dating.

Depth (cm)	Sample Type	^{14}C age ± error	Status	Modeled date (CE)
108	Plant/Wood	145 ± 20	Accepted	1818
214	Plant/Wood	235 ± 15	Accepted	1621
304	Plant/Wood	450 ± 15	Accepted	1403
368	Plant/Wood	815 ± 15	Accepted	1173
445	Plant/Wood	1230 ± 15	Accepted	733

stand for ~21 days. ^{210}Pb, ^{137}Cs, and ^{226}Ra activities were measured by gamma counting using an EG&G Ortec germanium detector (Schelske et al., 1994). Uppermost (0–100 cm) deposits in core LI2 were counted at 3-cm intervals. Two age-depth relations were developed for the core. The first used the constant rate of supply (CRS) ^{210}Pb model, which assumes that atmospheric (unsupported) ^{210}Pb was delivered to the sediment at a constant rate over the last 100–150 years (Goldberg, 1963; Krishnaswamy et al., 1971; Appleby and Oldfield, 1978). The second was developed utilizing the ^{137}Cs peak at 69–72 cm, which identifies the 1963 peak in atmospheric atomic bomb testing. We assumed a constant, linear sediment accumulation rate from that date to the top of the core, and extrapolated that mean rate to a core depth of 100 cm. We did not date core LI1 using ^{210}Pb and ^{137}Cs because of its proximity to dated core LI2. Instead, we assumed a sediment accumulation rate for LI1 that was the same as that derived for LI2.

Six wood fragments for AMS radiocarbon analysis were collected from core LI2 (Table 2) and five were collected from core LI3 (Table 3). Samples were washed using deionized water and submitted to the National Ocean Sciences Accelerator Mass Spectrometry (NOSAMS) Facility at Woods Hole Oceanographic Institution. Radiocarbon dates were calibrated using the IntCal13 calibration curve (Reimer et al., 2013). Age-depth models for cores LI2 and LI3 were developed with Bayesian statistics, utilizing the Bacon version 2.2 package in R® (Blaauw and Christen, 2011).

X-ray fluorescence (XRF) scanning for measures of Pb, Zn, and Ni was carried out at the University of Minnesota Duluth, using an ITRAX XRF core scanner with a Cr source tube at 30 kV and 55 mA, at 0.5-cm resolution with a 15-second dwell time. X-radiographs of the cores were collected using a Cr source tube running at 60 kV and 30 mA, with variable exposure times adjusted to the density of the sediments. Subsamples from the MWI cores were homogenized and placed in 2-cm^3 plastic containers and scanned at 1-mm resolution to obtain ~20 measurements per sample. A Cr source tube was utilized at 30 kV and 55 mA, with a 15-second dwell time. To constrain XRF measures and obtain quantitative results, concentrations of Pb, Zn, and Ni in subsamples were quantified using a Perkin Elmer AVIO 200 Inductively Coupled Plasma Optical Emission Spectrometer (ICP-OES) at the Center for Research in Energy and Environment at Missouri S&T. Subsamples were selected based on XRF results and core chronology, focusing mainly on the last 50 years. We conducted ICP-OES analysis on six samples from the uppermost part of core LI1 (between 0 and 42 cm) and eight samples from the uppermost part of core LI3 (between 0 and 51 cm). For core LI2, we analyzed 20 samples throughout the core, focusing on the section where major changes occur (60–125 cm). Samples were dried at 90 °C for 8 h. About 0.5 g of ground sediment was weighed into a 50-mL polypropylene container with 2 mL of HNO_3 (50%), 2 mL of HCl (20%) and 2 mL of H_2O_2 (30%). The contents were heated in a hot block at 90 °C for 1 h following the EPA 200.7 method for determination of metals in sediment samples (EPA, 1991).

Once samples were partially digested, they were cooled and filtered through a Thermo Scientific 0.45-μm Polytetrafluoroethylene (PTFE) filter. Mono-element standard solution (1000 ppm) for each element was diluted in 2% HNO_3 to prepare a multi-element (Pb, Zn, and Ni) calibration curve that ranged from 0.1 to 100 mg/L. The ICP-OES was calibrated with a four-point curve. All reagents were of the highest quality (i.e. trace metal grade, SupraPUR®) and all dilutions were made with high-purity water (18.2 mΩ/cm). For quality control, reagent blanks were used and replicate samples were analyzed every 14 samples. Heavy metal concentrations represent the average of three measurements. Matrix spike recovery was 103%.

2. Results

2.1. *Chronology*

2.1.1. *Core LI2*

Total ^{210}Pb activity in core LI2 declines with depth from the top of the core to a depth of 100 cm (Fig. 2A; Obrist-Farner et al., 2019). ^{226}Ra activity, however, displays a general decrease from 0 to 70 cm, but then increases from 70 to 100 cm. ^{226}Ra

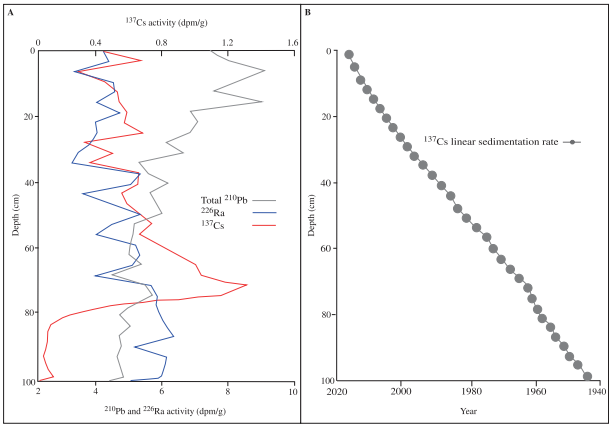

Fig. 2 – (A) ^{137}Cs, total ^{210}Pb and ^{226}Ra activities versus depth for core LI2. The ^{137}Cs peak occurs at 72 cm depth. (B) Linear sedimentation model, utilizing the ^{137}Cs peak and assuming a constant linear sedimentation rate from the peak to the top of the core and extrapolated to 100 cm. Modified from Obrist-Farner et al. (2019). (For interpretation of the references to color in this figure legend, the reader is referred to the web version of this article.)

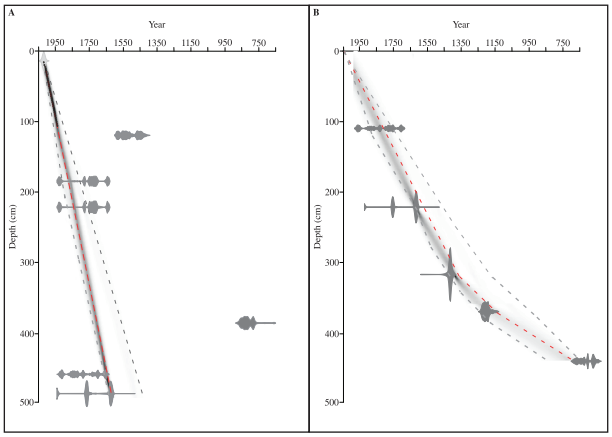

Fig. 3 – (A) Core LI2 age-depth model based on four calibrated ^{14}C dates, the ^{137}Cs peak, and the date of core retrieval (2017). Modified from Obrist-Farner et al. (2019). Red line shows the weighted mean age-depth model used in this study. Black dotted line from the surface to a depth of 100 cm represent age-depth model using ^{137}Cs. (B) The LI3 age-depth model based on five ^{14}C dates and the date of core retrieval (2017). Red line shows the weighted mean age-depth model used in this study. (For interpretation of the references to color in this figure legend, the reader is referred to the web version of this article.)

activity exceeds total ^{210}Pb activity in the core section from 70–100 cm, indicating disequilibrium between the two radionuclides. ^{210}Pb dates derived from the CRS model are inconsistent with the 1963 ^{137}Cs peak at 69–72 cm (Fig. 2A). The ^{210}Pb date at 72 cm is ~1900 CE, suggesting a ~60-year discrepancy between the dates from the two radionuclides. We opted to use the ^{137}Cs peak to date the core, for two reasons. First, downcore disequilibrium between ^{226}Ra and ^{210}Pb is evident and may contribute to dating uncertainty higher in the core (Brenner et al., 2004). Second, the ^{137}Cs date for onset of rises in Pb and Zn concentrations in core LI2 is consistent with the historical record of mining in the watershed. We thus used the ^{137}Cs-based chronology to assess recent changes through time in cores LI2 and LI1.

Samples from 112 and 394 cm in core LI2 yielded anomalously old ^{14}C ages (Table 2; Obrist-Farner et al., 2019) and were not used in the age-depth model. We ultimately utilized four ^{14}C dates, the ^{137}Cs peak at 72 cm, and the year of core collection (2017 CE) to constrain the age-depth model. The resulting model (Fig. 3A) yields a linear sedimentation rate that is almost constant, ~1.4 cm/yr. The bottom of the core has a weighted mean date of 1660 CE, with a 2σ date range of 1550–1679 CE (Fig. 3A; Obrist-Farner et al., 2019). Results from the LI2 core are discussed with respect to the weighted mean dates from the age-depth model.

2.1.2. *Core LI3*

Dates on terrestrial wood from the LI3 core were all in stratigraphic order and basal sediments are older than bottom deposits in core LI2 (Table 3). We used five ^{14}C dates and the year of core collection, i.e. the top of the core (2017 CE), to constrain the age-depth model. The resulting model (Fig. 3B) displays three mean sedimentation rates. From the bottom of the core at 455 cm (~730 CE) to 300 cm depth (~1400 CE), the linear sedimentation rate was 0.33 cm/yr (Fig. 3B). The sedimentation rate from 300 to 200 cm (~1650 CE) was 0.38 cm/yr. From 200 cm to the top of the core (2017 CE), the sedimentation rate was ~0.5 cm/yr. We describe results from the LI3 core with respect to weighted mean dates generated by the age-depth model (Fig. 3B).

2.2. *Core description*

2.2.1. *Core LI1*

The LI1-MWI core consists of gray mud that is rich in organic debris, with some intervals containing silty and sandy red mud. The consolidated part of the core (133–45 cm) can be subdivided into two parts. The lower part, from 133 to 80 cm (~1922–1959 CE) is sandy, with very coarse to coarse sand and granules. A thin bed of clay from 103 to 101 cm (~1943–1945 CE) separates the sandy interval in two. Both sandy intervals are moderately to poorly sorted and contain abundant lithic and mica grains. The sandy interval has higher density and magnetic susceptibility (MS) values than those observed in the muddy interval above (Fig. 4). The upper part of the consolidated segment, from 80 to 45 cm (~1959 to 1987 CE), is characterized by gray, sometimes laminated mud, with macroscopic organic debris and woody material. The interval contains laminae and thin beds, as seen in radiographic images. Density and MS values in this interval are low, with some particularly low-density values where there are abundant organic fragments (Fig. 4).

2.2.2. *Core LI2*

The LI2-MWI core consists of gray to dark gray mud, with intervals of olive to olive-gray mud. The consolidated part of the core can be subdivided into four parts. The deeper part, from 505 to 260 cm (~1660–1810 CE), is composed of dark, olive-gray to very dark gray silty mud. The interval is characterized by a uniform, massive structure, with scattered laminae and thin beds, as seen in radiographic images. Density and MS show small variations throughout the interval (Fig. 5). From 260 to 203 cm (~1810–1850 CE), the sediment is composed of dark gray and olive mud. Thick laminations and thin beds are common and apparent in the radiographic images (Fig. 5). Density and MS show several pronounced peaks in this interval (Fig. 5). From 203 to 192 cm (~1850–1860 CE), the core is com-

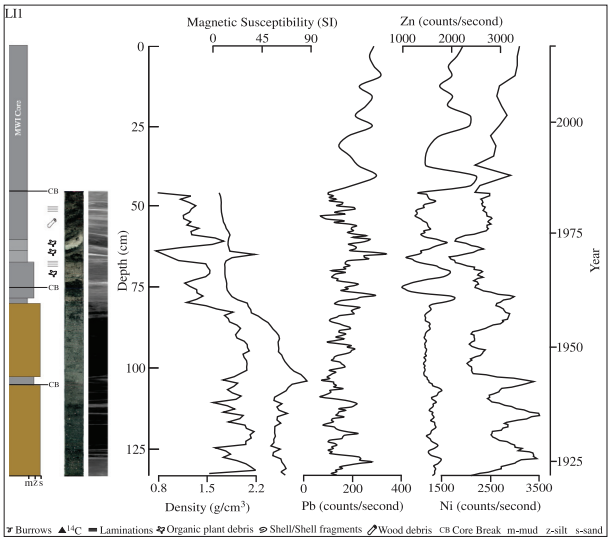

Fig. 4 – Core description, core photograph, density, magnetic susceptibility, and Pb, Zn and Ni XRF profile for LI1. Note the high Ni and the relatively constant Pb and Zn values.

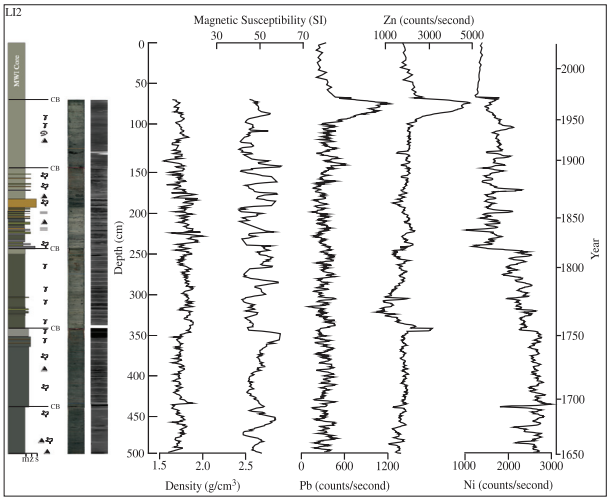

Fig. 5 – Core description, core photographs, density, magnetic susceptibility and Pb, Zn and Ni XRF profile for the LI2 core, modified from Obrist-Farner et al. (2019). Up-core increases in Pb and Zn indicate a deviation from background levels that occurred between 1945 and 1965, suggesting an anthropogenic source of Pb and Zn. For legend, see Fig. 4.

posed of light olive-brown, medium-to-coarse muddy sand. Sand grains are sub-rounded to rounded, and the interval is moderately well sorted, with no clear grain-size trend. Density and MS are highly variable in this interval, with higher values than those observed above (Fig. 5). The uppermost part, from 192 to 70 cm (~1860–1965 CE), is composed of olive gray mud with intervals that are rich in plant remains. The interval appears to be mottled and contains small, broken shell fragments. Density and MS values vary throughout the interval (Fig. 5) and radiographic images show laminations and thin to medium beds in this core segment (Fig. 5).

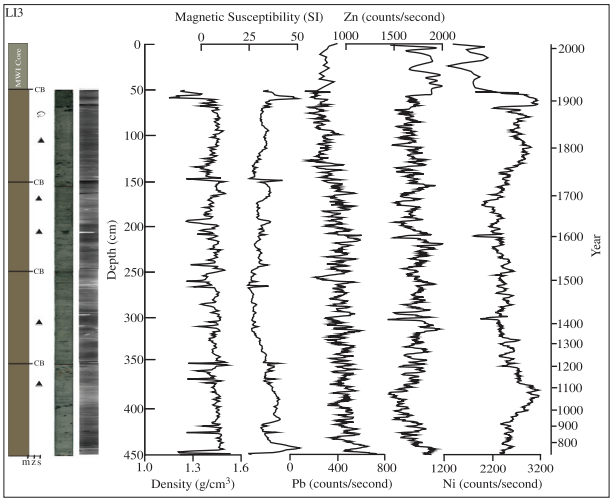

Fig. 6 – Core description, core photograph, density, magnetic susceptibility, and Pb, Zn and Ni XRF profile for LI3. Metal values remain relatively constant throughout the core. For legend, see Fig. 4.

2.2.3. *Core LI3*

The deeper part of the LI3-MWI core, from 455 to 51 cm (~750–1923 CE), is composed of homogenous mud, with silty and sandy intervals. Organic debris is common throughout this part of the core. Some intervals appear to be thinly laminated, as is evident in radiographic images (Fig. 6). The radiographic images indicate that the core contains laminations and thin to medium beds, which were not evident during visual inspection of the core. The uppermost part of the LI3-MWI core is characterized by gray to olive-gray mud (51–0 cm; ~1923–2017 CE).

2.3. *Core geochemistry*

Element abundances, measured by XRF scanning of the three cores, display a wide range of values. We focus on the relative abundances (XRF scans) and concentrations (ICP-OES) of Pb, Zn, and Ni because these elements are the targets of mining operations in the Lake Izabal catchment.

2.3.1. *Core LI1*

Pb, Zn, and Ni profiles display different trends (Fig. 4). Pb shows large variability throughout the core, with relative abundances ranging from 50 to 350 counts per second (c/s). Zn is relatively constant in the lower, sandy portion of LI1 (Fig. 4). In the muddy interval, however, Zn is highly variable, displaying several peaks and troughs. Overall, values range from 1000 to 2500 c/s. Ni relative abundance displays high variability throughout the core. Highest values were measured in the lower, sandier section of the core, with values ranging from 2300 to 3300 c/s. Thereafter, Ni values decrease, with values typically ranging from 1600 to 2000 c/s. Higher values, ranging from 2500 to 3000 c/s, occur again from 45 cm (~1985 CE) to the top of the core.

ICP-OES results are similar to XRF results in the upper 42 cm of the core (~1987 CE). Pb increases from 20 to 38 parts per million (ppm) between the sample at 42 cm and the sample at the surface. This up-core increase is also observed in both the Zn and Ni concentrations, which show enrichment from the deepest to the uppermost sample. Zn increases from a low of 75 ppm at 39 cm (~1989 CE) to a high of 124 ppm at the

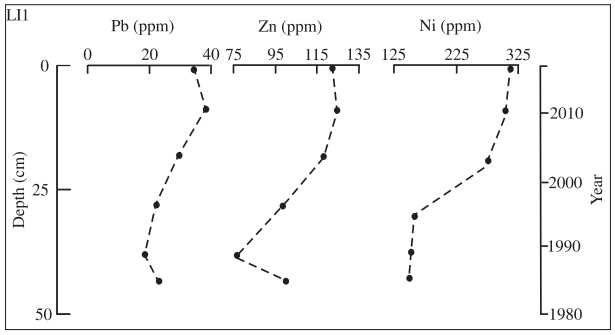

Fig. 7 – Pb, Zn, and Ni concentrations in the LI1 core. Notice the increase in Ni concentration in the upper 30 cm of the core. There is also a slight increase of Pb concentration in the upper part of the core that deviates from background levels.

surface. Ni increases from a low of 147 ppm at 42 cm to a high of 309 ppm at the surface (Fig. 7).

2.3.2. *Core LI2*

The XRF profiles for Pb, Zn, and Ni show distinct trends in the LI2 core. Both the Pb and Zn relative abundances are constant from the bottom of the core to a depth of 100 cm (~1945 CE).

From 100 cm to 70 cm (~1965 CE), there is a dramatic increase in relative abundance for both elements. Pb changes from 300 to 1200 c/s and Zn changes from 1800 c/s to almost 5000 c/s. Both Pb and Zn decrease back to lower values above 70 cm, similar to counts observed in the lower part of the core. Ni abundance, on the other hand, shows three general trends throughout the core. From the bottom of the core (505 cm; ~1660 CE) to a depth of 250 cm (~1818 CE), the relative abundance of Ni remains relatively constant, with an average of 2500 c/s, and just a few pronounced peaks. Thereafter, there is an increasing trend in relative abundance from 250 cm (~1818 CE) to 70 cm (~1965 CE), with several peaks that range between 800 and 2300 c/s. Variability in this interval is high. Ni content is relatively constant (~1200 c/s; Fig. 5) from 70 cm (~1965 CE) to the top of the core.

Concentrations obtained via ICP-OES are similar to relative abundances obtained by XRF (Fig. 8). Concentrations of Pb and Zn are relatively low and stable in the lower part of the core, up to a depth of 100 cm (~1945 CE). Pb and Zn concentrations increase substantially between 100 and 70 cm (~1945–1965 CE), to 329 mg/kg and 332 mg/kg, respectively. From 70 cm to 0 (~1965–2017 CE), average concentrations of Pb (~80 mg/kg) and Zn (~160 mg/kg) decrease and reach similar concentrations as those observed in the lower part of the core. ICP-OES-derived Ni concentrations, on the other hand, display several peaks and troughs that are not observed in the XRF data. From the bottom of the core (505 cm; ~1660 CE) to a depth of 100 cm, the concentrations remain relatively constant, between 125 and 160 mg/kg, but a sharp increase to 190 mg/kg occurs at 105 cm (~1934 CE). There is an increase in the concentration of Ni from 80 cm (~1959 CE; 100 mg/kg) to the top of the core (160 mg/kg) (Fig. 8).

2.3.3. *Core LI3*

The XRF profiles for Pb, Zn and Ni show distinct trends in the LI3 core (Fig. 6). Pb relative abundance displays several peaks, and values throughout the core range between 150 and 740 c/s. Zn relative abundances decrease rapidly from the bottom of the core to a depth of 51 cm (~1923 CE), after which Zn shows the highest values to the surface (~2017 CE; ~2000 c/s). Several

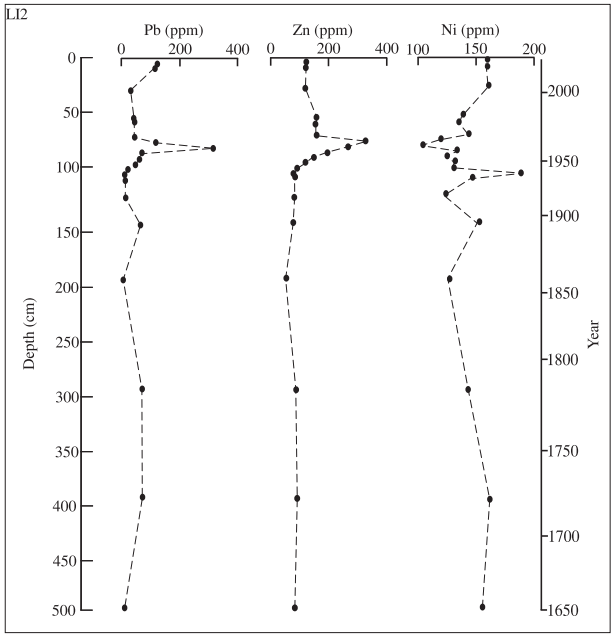

Fig. 8 – Concentrations of Pb, Zn and Ni, analyzed via ICP-OES, in core LI2. Large changes between 100 and 70 cm occur at the same depths where large shifts were detected by XRF analyses.

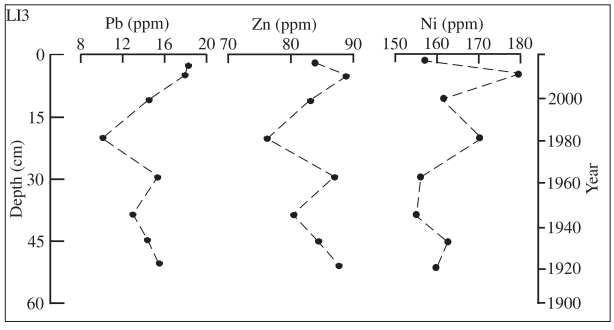

Fig. 9 – Concentrations of heavy metals (Pb, Zn and Ni), analyzed via ICP-OES, in the upper part of core LI3.

high values, however, were measured at depth in the profile and are comparable to those in the surface sediment (~2000 c/s). Variability in Ni relative abundance is greater than that for Pb and Zn throughout the core. Values between 455 cm (~720 CE) and 71 cm (~1886 CE) are variable, with relative abundance of Ni ranging between 1800 and 3200 c/s. Thereafter, there is a sharp increase (3100 c/s) at 65 cm (~1900 CE). The topmost part of the core (50–0 cm) has values ranging between 1300 and 2000 c/s.

Concentrations of Pb and Zn (Fig. 9) in the upper part of the core, from 51 to 0 cm (~1923–2017 CE), are variable and lower than values observed at the other two study locations. The highest Pb concentration was obtained at the surface (17 mg/kg), whereas the highest concentration of Zn was obtained at 3 cm (89 mg/kg). Ni concentration increases above 30 cm in the core (~1962 CE; 157 mg/kg), with the highest concentration observed at 6 cm (~2006 CE; 180 mg/kg).

3. Discussion

Relative abundances and concentrations of Pb, Zn, and Ni in the three cores from Lake Izabal suggest recent heavy metal contamination of the sediment, especially during the last ~60–70 years. Data from the three cores indicate that point sources contributed to higher metal concentrations in the lake sediments, near to where such metal contamination entered the lake, and that spatial redistribution of metals in the lake was minimal. Redistribution probably did not occur because Lake Izabal is a freshwater, mildly alkaline lake (pH 7.5–8.4; Dix et al., 1999), making galena (7.4–7.6 g/cm^3), sphalerite (3.9–4.2 g/cm^3), and garnierite (1.56–1.6 g/cm^3) particles, the dominant hosts of Pb, Zn, and Ni in the area, insoluble (Daskalakis and Helz, 1993; Liu, et al., 2007; Wells et al., 2009). Furthermore, these minerals are denser than other minerals in the sediment cores (e.g., quartz), resulting in rapid deposition. High sediment accumulation rates, as measured in LI2 (~1.4 cm/yr) and inferred for LI1, bury such metal particles rapidly, reducing the likelihood of redistribution. XRF profiles for LI1 indicate that metal abundances in the area remained fairly constant for the last ~100 years, especially for Pb and Zn. High abundance of Ni in the lower sandy interval of LI1 is interpreted to represent a time of greater erosion from the northern mountain range, where there are Ni-rich laterite deposits. Similar abundances of Ni are not observed again until the uppermost, muddy part of the core, indicating a possible increase in Ni delivery. The recent increase correlates temporally to the onset of Ni mining in the Lake Izabal area. This increase is also observed in the ICP-OES results, which show that higher amounts of Ni began accumulating in the area between ~1999 and 2007 CE, reaching a maximum of 310 ppm today. Temporal correlation of Ni mining in the area and upward increase in Ni concentration in LI1 might be a coincidence because similar Ni abundance is observed in the lower (pre-mining) and upper parts of the LI1 core. By examining sediments along the north shore of Lake Izabal, far from the Ni mine (Fig. 1B), it may be possible to determine if the increase in Ni is restricted to the area near the mine, or if rivers that drain the lateriterich soils of the northern mountain range are responsible for increasing Ni concentration in the lake.

XRF profiles for LI2 also show changes in heavy metal abundances and concentrations. Pb and Zn abundances are relatively constant throughout the core, but increase between ~1945 and 1965 CE. Such increases are also observed in ICP-OES-measured concentrations, which show Pb increased from 79 to 329 ppm, and Zn from 115 to 332 ppm in the 20-year interval. High levels indicate rapid, high input of metals from the catchment to the lake, and their delivery to the core site near the Polochic Delta. Temporal correlation between high Pb and Zn concentrations in the core and activation of the Caquipec mine near the Cahabon River (Machorro, 1996; ICEFI, 2014) suggests a cause-and-effect relation between the two. If so, the Cahabon River was probably severely contaminated during metal extraction at the mine site near Coban.

Ni abundance in LI2, on the other hand, shows no such recent increase in concentration (Fig. 5). Furthermore, ICP-OES-derived concentrations (Fig. 8) differ from the XRF results (Fig. 5), the former remaining fairly close to ~150 ppm and showing a slight decrease between ~1945 and 1965 CE. XRF profiles for the three studied metals in LI3, i.e. the "control core," show little variation through time. Such data indicate that metals from point sources did not reach the southern shore of Lake Izabal, i.e. that distant transport or redistribution of metals from point sources did not occur.

Previous studies demonstrated the utility of analyzing sediment cores to establish background levels of heavy metals (Iskandar and Keeney, 1974; Callender and Van Metre, 1997; Heyvaert et al., 2000; Guyard et al., 2007). The studies of Machorro (1996), Oliva (2005), and Oliva et al. (2010) in Lake Izabal showed that metals are abundant in the lake sediments, but those studies lacked the historical perspective provided by sediment core data, which are needed to determine if high metal concentrations were caused by bedrock erosion or anthropogenic activities. High precipitation in the region (Perez et al., 2011), coupled with diverse mineral deposits and bedrock lithology (Bonis et al., 1970; Bartole et al., 2019), can lead to high metal concentrations in the sediments of downstream lakes, simply because of erosion. Metal concentrations we found in sediment cores from Lake Izabal, in particular Pb and Zn, are similar to those found in surface sediments from the lake by Machorro (1996), Oliva (2005) and Oliva et al. (2010). Concentrations of Ni in surface sediments found by Machorro (1996; 227 ppm), and those measured in the LI1 core, are higher than values ~25 years ago and indicate that recent, ongoing Ni extraction north of Lake Izabal has increased Ni in recent deposits. Alternatively, the recent increase in concentration is a result of increased erosion in the northern mountain range and natural erosion has increased Ni in the lake sediments (as suggested by values in bottom sediments from LI1). Furthermore, insolubility of garnierite ore in water (Wells et al., 2009) leads to preferential deposition of Ni near the processing plant (i.e. near the LI1 core site), which prevents its distribution throughout the lake, as evident from the relatively low Ni concentrations in recent LI2 and LI3 sediments. Examining lake sediments from sites near inflows of rivers that drain the northern, Ni-rich mountain range, can provide a clearer picture of the role of anthropogenic activities on Ni enrichment in sediments of Lake Izabal and their potential to be redistributed in the lake.

Concentrations of Pb and Zn in the three study cores probably reflect natural erosion of bedrock, especially because amounts in sediments have remained constant for >100 years in LI1, ~350 years in LI2, and ~1200 years in LI3. Furthermore, there is no upward increase in metal concentrations that could be linked to population growth, i.e., from greater wastewater discharge (Figs. 7, 8 and 9). This finding is in contrast to other studies that show metals have increased in lacustrine systems in response to wastewater discharge into their inflow tributaries (Ioannides et al., 2015). It is possible that the wetland on the west side of Lake Izabal acts as a sink, sequestering nutrients and metals that would otherwise enter Lake Izabal (Dix et al., 1999; Obrist-Farner et al., 2019).

Pb and Zn concentrations in cores LI1 and LI3 and most of core LI2, as well as surface sediments from Lake Izabal (Machorro, 1996; Oliva, 2005; Oliva et al., 2010), are significantly lower than those measured in sediments from the section of core LI2 deposited between ~1945 and 1965 CE. Those high concentrations in core LI2 correlate temporally with galena and sphalerite extraction in the Coban region (Fig. 1) ~70 years ago (Roberts and Irving, 1957; Van Wouw and Minaar, 2013). Concentrations in LI2 during that time are very high and indicate that contamination of the Cahabon River during the 20 years of mining was substantial. The high levels are somewhat surprising because it has been shown that heavy metal concentrations decrease substantially with distance from mining operations (Rosner, 1998). Pb and Zn contamination in Lake Izabal, ~120 km from the Caquipec mine, shows the potential for contaminants to travel large distances from source areas.

Poor management and lax regulations regarding environmental monitoring during mining operations have hampered the ability of investigators to assess contamination in Lake Izabal. The studied sediment cores provide estimates of background metal concentrations in Lake Izabal and confirm that high heavy metal concentrations in surface sediments were caused by human activities.

Although XRF-derived metal profiles are useful, the cause of some stratigraphic changes is hard to discern. Changes in the XRF profiles, especially Ni abundance in LI2 and in the upper part of LI3 (Zn and Ni abundance), do not correlate well with concentrations obtained by ICP-OES. Such discrepancies can be the result of water content in the sediment cores, which has been shown to affect XRF results (Tjanllingii et al., 2007). It is unclear why abrupt changes in Ni abundance occur in LI2, but changes in the upper part of LI3 could result from high water content in the MWI core samples. Despite the potential confounding of XRF-derived metal abundance by water, the combination of XRF analyses and ICP-OES measurements is a powerful method to establish background metal levels and evaluate the source(s) of recent, high heavy metal concentrations (Audry et al., 2004; Chawchai et al., 2015; Jimenez-Arias et al., 2016).

The United States Environmental Protection Agency (EPA) established a limit of 15 parts per billion (ppb) Pb in drinking water and 400 ppm in soils (EPA, 2005; ATSDR, 2017; EPA, 2019). Although Pb concentrations in sediments in core LI2 are not that high, the fact that such high concentrations are found ~120 km from the source is reason for concern. The Cahabon River joins the Polochic River before entering Lake Izabal, crossing a wetland that local inhabitants use to cultivate crops. EPA established ecological soil screening levels (ECO-SSLs) that protect biota that live in soils contaminated by metals (EPA, 2007a, 2007b). Levels in Lake Izabal sediments are higher than those recommended for ECO-SSLs, especially Pb and Zn amounts in core LI2, near the Polochic Delta. Future studies should focus on the sediments of the wetland, especially zones adjacent to the Polochic and Cahabon Rivers, to investigate possible soil contamination.

4. Conclusions

This paleolimnological study highlighted the role of natural erosion and mining activities on the concentrations of metals in sediments of Lake Izabal, Guatemala. Relative abundances and concentrations of Pb, Zn, and Ni in the cores are comparable to metal concentrations observed in previous studies. Diverse bedrock lithologies, including mafic igneous rocks and mineral-rich deposits in the lake catchment, are the reason for metal concentrations observed in the lake. Despite being ~120km away, activity at the Caquipec Mine correlates temporally to the increase in Pb and Zn observed between 1945 and 1965 in the core collected near the Polochic Delta. This observation suggests long-distance transport of metals. The Polochic wetland, an area periodically flooded by the Polochic and Cahabon Rivers, probably trapped large amounts of Pb and Zn between 1945 and 1965, and should be the focus of future studies to investigate possible soil contamination. The increase in Ni observed in the LI1 core correlates temporally to Ni mining operations in the Lake Izabal area, but natural erosion of bedrock cannot be ruled out as a possible source for such an increase. Increases in both Pb and Zn in the Polochic Delta, and Ni along the north shore of Lake Izabal, highlight the impact of point sources on metal concentrations in the lake. Metal redistribution, however, is apparently not a concern, at least at the western end of Lake Izabal, as shown by comparison of metal concentrations in the three cores. In the future, sediment cores from the east end and along the northern shore of Lake Izabal can be used to test this hypothesis. Results of this study provide estimates of natural, background metal concentrations, before anthropogenic activities began in the lake catchment. The results can inform future monitoring efforts dealing with contamination of the lake ecosystem, especially those caused by exploration and mining activities in the area.

Acknowledgments

E.H. thanks Missouri University of Science and Technology and a graduate student research grant from the Geological Society of America for support, and the Center for Research in Energy and Environment for help using the ICP-OES. We thank two anonymous reviewers who helped improve the quality of the manuscript, and Robert Brown at the University of Minnesota-Duluth for XRF core scanning and analysis. Finally, we are grateful to the Guatemalan NGO "Defensores de la Naturaleza," which facilitated work carried out in Lake Izabal in 2017. This is contribution # 4 from the Missouri S&T MCTF research group.

REFERENCES

Aldana, R., Abate, R., 2016. Banning metal mining in Guatemala. Vt. L. Rev. 40 (597), 1–75.
Appleby, P.G., Oldfield, F., 1978. The calculation of Lead-210 dates assuming a constant rate of supply of unsupported ^{210}Pb to the sediment. Catena 5, 1–8.
ATSDR, 2005. Public health statement. Zinc, CAS# 7440-66-6: agency for toxic substances and disease registry, 164.
ATSDR, 2017. Case studies in environmental medicine (CSEM). Lead Toxicity. Agency Toxic Subst. Dis. Regist. 185.
Audry, S., Schafer, J., Blanc, G., Jouanneau, JM., 2004. Fifty-year sedimentary record of heavy metal pollution (Cd, Zn, Cu, Pb) in the lot river reservoirs (France). Environ. Pollut. 132, 413–426.
Bansal, S., Ashtana, S., 2018. Biologically essential and non-essential elements causing toxicity in the environment. J. Environ. Anal. Toxicol. 8, 1–5.
Barrientos, C.A., 2005. Fish abundance and community composition in native and non-native littoral aquatic plants at Lake Izabal, Guatemala [MS Thesis: University of Florida], 41.
Bartole, R., Lodolo, E., Obrist-Farner, J., Morelli, D., 2019. Sedimentary architecture, structural setting, and Late Cenozic depocentre migration of an asymmetric transtensional basin: Lake Izabal, eastern Guatemala. Tectonophysics 750, 419–433.
Binimelis, R., Monterroso, I., Rodriguez-Labajos, B., 2007. A social analysis of the bioinvasions of *Dreissena polymorpha* in Spain and *Hydrilla verticillata*. Guatemala Environ. Manage. 40, 555–566.
Blaauw, M., Christen, J.A., 2011. Flexible paleoclimate age-depth models using an autoregressive gamma process. Bayesian Anal. 6 (3), 457–474.
Bonis, S., Bohnenberger, O.H., and Dengo, G.C., 1970. Mapa geológico de la República de Guatemala. Instituto Geografico Nacional. Scale 1:500,000 (in Spanish).
Bradl, H.B., 2005. Heavy Metals in the Environment: Origin, Interaction and Remediation Chapter 1 Sources and origins of heavy metals. Interface Sci. Technol. 6 (c), 1–27.
Brenner, M., Schelske, C.L., Kenney, W.F., 2004. Inputs of dissolved and particulate ^{226}Ra to lakes and implications for ^{210}Pb dating recent sediments. J. Paleolimnol. 32, 53–66.
Brezonik, P., Fox, J., 1974. The limnology of selected Guatemalan lakes. Hydrobiologia 45 (4), 467–487.
Brinson, M., 1973. The organic matter budget and energy flow of a tropical lowland aquatic ecosystem [PhD: University of Florida], 251 p.
Brinson, M., Nordlie, F., 1975. II. Lakes. 8. Central and South America: Lake Izabal, Guatemala.. Verh. Internat. Verein. Limnol. 19, 1468–1479.
Brocard, G., Bettini, A., Pfeifer, H.-R., Adatte, T., Moran-Ical, S., Gonneau, C., Vasquez, O., 2016. Eutrophication and chromiun contamination in Lake Chichoj, Alta Verapaz, Guatemala. RGCT 3, 1–21.
Bryan, G.W., Langston, W.J., 1992. Bioavailability, accumulation and effects on heavy metals in sediments with special referes to United Kingdom estuaries: a review. Environ. Pollut. 76 (2), 89–131.
Callender, E., Van Metre, P., 1997. Reservoir sediment cores show U.S. lead declines. Environ. Sci. Technol. 31 (9), 424–428.
Cempel, M., Nikel, G., 2006. Nickel: a review of its sources and environmental toxicology pol. J. Environ. Stud. 15 (3), 375–382.
Chatta, A., M., Khan, M.N., Mirza, S.Z., Ali, A., 2016. Heavy metal (Cadmium, lead, and chromium) contamination in farmed fish: A potential risk for consumers' health. Turk. J. Zool. 40, 1–9.
Chawchai, S., Kylander, M.E., Chabangborn, A., Lowemark, L., Wohlfarth, B., 2015. Testing commonly used X-ray fluorescence core scanning-based proxies for organic-rich lake sediments and peat. Boreas. 1–10.
Chu, Z., Yang, Z., Wang, Y., Sun, L., Yang, W., Yang, L., Gao, Y., 2019. Assessment of heavy metal contamination from penguins and anthropogenic activities on Fildes Peninsula and Ardley Island, Antarctic. Sci. Total Environ. 646, 951–957.

Daskalakis, K, Helz, G, 1993. The solubility of sphalerite (ZnS) in sulfidic solutions at 25 °C and 1 atm pressure. Geochim. Cosmochim. Acta. 57 (20), 4923–4931.
EPA, 1991. Methods for the determination of metals in environmental samples. USEPA-600/4-91-010, 293.
EPA, 2005. Ecological soil screening levels for lead: interim final. USEPA-OSWER Directive 9285.7–70, 76.
EPA, 2007a. ecological soil screening levels for nickel: interim final.USEPA-OSWER Directive 9285.7-76, 113.
EPA, 2007b. Ecological soil screening levels for Zinc: interim final. USEPA-OSWER Directive 9285.7-73, 781.
EPA, 2019. Hazard standards for lead in paint and soil (TSCA Section 403). https://www.epa.gov/lead/hazard-standards-lead-paint-dust-and-soil-tsca-section-403
Dix, A., Maldonado, M., Dix, M., Bocaletti, O., Giron, R., De La Roca, I., et al., 1999. Integridad Biologica del Lago de Izabal: Universidad del Valle de Guatemala, Centro de Estudios Ambientales. Informe Final, Proyecto 4, 133 (in Spanish).
Fisher, M., Brenner, M., Reddy, K., 1992. A simple, inexpensive piston corer for collecting undisturbed sediment/water interface profiles. J. Paleolimnol. 7, 157–161.
Goldberg, E., 1963. Geochronology with lead-210 in radioactive dating. In: Proceedings IAEA Symposium, Vienna, pp. 121–131.
Goldin, S., 2008. Suggested Practices to Reduce Zinc Concentrations in Industrial Stormwater Discharges, 34. Department of Ecology, State of Washington 08-10-025.
Goodman, J., Prueitt, R., Thakali, S., Oller, A., 2011. The nickel ion bioavailability model of the carcinogenic potential of nickel-containing substances in the lung. Inf. Healthc. 41 (2), 142–174.
Guyard, H., Chapron, E., ST-Onge, G., Anselmetti, F., Magand, O., Francus, P., et al., 2007. High-altitude varve record of abrupt environmental changes and mining activity over the last 4000 years in the Western French alps (Lalke Brament, Grandes Rousses Massif). Quat. Sci. Rev. 26, 2644–2660.
Harju, H., 1979. Exploration of exmibal's nickel laterite deposits in Guatemala. In: Proceedings Laterite Symposium, Toronto, pp. 245–524.
Heyvaert, A., Reuter, J., Slotton, D., Goldman, C., 2000. Paleolimnological reconstruction of historical atmospheric lead and mercury deposition at Lake Tahoe, California – Nevada. ES&T 34, 3588–3597.
ICEFI-Instituto Centromericano de Estudios Fiscales, 2014. La minería en Guatemala: Realidad y desafios frente a la democracia y el desarrollo, p. 82 (in Spanish).
Ioannides, K., Stamoulis, D., Papachristodoulou, C., Tziamou, E., Markantonaki, C., Tsodoulos, I., 2015. Distribution of heavy metals in sediment cores of Lake Pamvotis (Greece): a pollution and potential risk assessment. Environ. Monit. Assess. 187 (4209), 1–16.
Iskandar, K., Keeney, D., 1974. Concentration of heavy metals in sediment cores from selected Wisconsin lakes. ES&T 8 (2), 165–170.
Jaishankar, M., Tseten, T., Anbalagan, N., Mathew, B., Beeregowda, K., 2014. Toxicity, mechanism and health effects of some heavy metals. Interdiscip. Toxicol. 7 (2), 60–72.
Jimenez-Arias, J., Mata, M., Corzo, A., Poulton, S., Marz, C., Sanchez-Bellon, A., et al., 2016. A multiproxy study distinguishes environmental change from diagenetic alteration in the recent sedimentary record of the inner Cadiz Bay (SW Spain). Holocene 26, 1355–1370.
Krishnaswamy, S., Lal, D., Martin, J.M., Meybeck, M., 1971. Geochronology of lake sediments. Earth Planet. Sc. Lett. 11, 407–414.
Liu, J., Jinschek, J.R., Hochella, J., 2007. Invetigation of the Aqueous Dissolution of Galena (PbS) nanoparticles by HRTEM. Micros. Microanal. 13 (S02), 516–517.
Livingstone, D.A., 1955. A lightweight piston sampler for lake deposits. Ecology 36 (1), 137–139.
Machorro, R., 1996. Water Quality at Lago de Izabal, Guatemala: Geochemical characterization and assessment of trophic status [PhD: University of Texas], 240.
Martin, S., Griswold, W., 2009. Human health effects of heavy metals: environmental science and technology briefs for citizens. Center Hazardous Subst. Res. 15, 1–6.
McIlveen, W., Negusanti, J., 1994. Nickel in the terrestrial environment. Sci. Total Environ. 148 (2-3), 109–138.
Medina, C., Gomez-Enri, J., Villares, P., Alonso, J., 2009. An Integrated Methodology for the Environmental Assessment and Management of Lake Izabal (Guatemala). In: Proceedings Proceedings of the 3rd WSEAS Int. Conf. on Energy Planning, Energy Saving, Environmental Education, pp. 150–157.
Michot, T., Boustany, R.G., Arrivillaga, A., Perez, B., 2002. Impacts of hurricane mitch on water quality and sediments of Lake Izabal, Guatemala. USGS 20.
Needleman, H.L., 1998. Clair Patterson and Robert Kehoe: two views of lead toxicity. Environ. Res. 78, 79–85.
Nriagu, J.O., Pacyna, J., 1988. Quantitative Assessment of Worldwide Contamination of Air, Water and Soil by Trace Metals. Nature 333, 134–139.
Obrist-Farner, J., Brenner, M., Curtis, J.H., Kenney, W., Salvinelli, C., 2019. Recent onset of eutrophication in Lake Izabal, the largest water body in Guatemala. J. Paleolimnol. 62, 359–372.
Oliva, B., 2005. Contaminacion en el lago de Peten Itza. Final report No. 20-2002. CONCYT. 115 (in Spanish).
Oliva, B., 2007. El Pez Blanco (*Petenia splendida*) y la contaminacion en el lago Peten Itza. Final report No. 49-2005. CONCYT. 123 (in Spanish).
Oliva, B., Perez, J., Herrera, K., Gaitan, I., Callejas, B., Osorio, C., Martinez, O., Mardoqueo, A., Hernandez, J., 2010. Evaluación de la contaminación fisico-quimica y bateriológica en el agua del Rio Dulce y Lago de Izabal, p. 118 Final report No. 025-2006. CONCYT(in Spanish).
Perez, L., Bugja, R., Massaferro, J., Steeb, P., Van Geldern, R., Frenzel, P., et al., 2010. Post-Columbian environmental history of Lago Peten Itza, Guatemala Rev. Mex. Cienc. Geol. 27, 490–507.
Perez, L., Frenzel, P., Brenner, M., Escobar, J., Hoelzmann, P., Scharf, B., Schwalb, A., et al., 2011. Late Quaternary (24-10 ka BP) environmental history of the Neotropical lowlands inferred from ostracodes in sediments of Lago Peten Itza, Guatemala. J. Paleolimnol. 46, 59–74.
Perez, F., Hernandez, E., Valladares, B., 2014. Evaluacion de contaminantes emergentes y radiactivos en el lago de Atitlan, p. 54 Final report. USAC-DIGI(in Spanish).
Rathor, G., Chopra, N., Adhikari, T., 2014. Nickel as a pollutant and its management. Int. Res. J. Environ. Sci. 3 (10), 1–5.
Reimer, P., Bard, E., Bayliss, A., Warren, J., Blackwell, P., Bronk, C., et al., 2013. Intcal 13 and marine 13 radiocarbon age calibration curves 0-50,000 years cal BP. Radiocarbon 55 (4), 1869–1887.
Rengberg, I., Wik-Persson, M., Emteryd, O., 1994. Pre-industrial atmospheric lead contamination detected in Swedish lake sediments. Lett. Nat. 368, 630–634.
Rosner, U., 1998. Heavy metals in surface soils and streambed sediments in the Wallapai Mining. District, Northwestern Arizon, A Historic Mining Distric in a Semiarid Region. Arizona Geological Survey Report CR-98-A, 46.
Roberts, R., Irving, E., 1957. Mineral Deposits of Central America. Geological Survey Bulletin 1034. U.S. Government Printing Office, p. 220.
Schelske, C.L., Peplow, A., Brenner, M., Spencer, C.N., 1994. Low-background gamma counting: applications for ^{210}Pb dating of sediments. J. Paleolimnol. 10, 115–129.
Tao, Y., Yuan, Z., Xiaona, H., Wei, M., 2012. Distribution and bioaccumulation of heavy metals in aquatic organisms of different trophic levels and potential health risk assessment from Taihu lake, China. Ecotox. Environ. Safe 81, 55–64.
Tchounwou, P., Yedjou, C., Patlolla, A., Sutton, D., 2012. Heavy metals toxicity and the environment. NIH-PA 101, 133–164.
Thevenon, F., Graham, N.D., Chiaradia, M., Arpagaus, P., Wildi, W., Pote, J., 2011. Local to regional scale industrial heavy metal pollution recorded in sediments of large freshwater lakes in central Europe (lakes Geneva and Lucerne) over the last centuries. Sci. Total Environ. 412-413, 239–247.
Thyssen, J., Johanse, J., Menne, T., 2007. Contact allergy epidemics and their controls. J. Compil. 56, 185–195.
Tjanllingii, R., Rohl, U., Kolling, M., Bickert, T., 2007. Influence of the water contect on X-ray fluorescence core-scanning measurements in soft marine sediments. Geochem. Geophys. Geosys. 8 (2), 1–12.
Van Wouw, K., Minaar, A., 2013. Canadian National Instrument 43-101 Technical Report. Preliminary Economic Assessment Guatemala. Canadian National Instrument 43-101 Technical Report. Preliminary Economic Assessment Guatemala, 136. Torlon Hill Project.
Wells, M., Ramanaidou, E., Verrall, M., Tessarolo, C., 2009. Mineralogy and crystal chemistry of "garnierites" in the Goro lateritic nickel deposit, new Caledonia. Eur. J. Miner. 21, 167–483.
WHO, 2005. Nickel in drinking-water: Backgroung document for development of WHO guidelines for drinking-water Quality. 30.